AGU PUBLICATIONS

JGR

Journal of Geophysical Research: Atmospheres

RESEARCH ARTICLE

10.1002/2014JD022959

Key Points:
- Improved diagnostic of hail events in climate models by logistic regression
- Logistic hail model shows good agreement with observed hail events
- Potential for hail events will be slightly increasing in some parts of Germany

Correspondence to:
S. Mohr,
mohr@kit.edu

Citation:
Mohr, S., M. Kunz, and K. Keuler (2015), Development and application of a logistic model to estimate the past and future hail potential in Germany, *J. Geophys. Res. Atmos.*, *120*, 3939–3956, doi:10.1002/2014JD022959.

Received 15 DEC 2014
Accepted 4 APR 2015
Accepted article online 10 APR 2015
Published online 12 MAY 2015

Development and application of a logistic model to estimate the past and future hail potential in Germany

S. Mohr[1,2], M. Kunz[1,2], and K. Keuler[3]

[1]Institute of Meteorology and Climate Research (IMK-TRO), Karlsruhe Institute of Technology, Karlsruhe, Germany, [2]Center for Disaster Management and Risk Reduction Technology, Karlsruhe and Potsdam, Germany, [3]Chair Environmental Meteorology, Brandenburg University of Technology Cottbus-Senftenberg, Cottbus, Germany

Abstract This study investigates to what extent the frequency of hail events in the summer months has changed during the past decades and which changes are expected to occur in the future. To improve the diagnostics of hail events by considering various factors relevant for the formation of hail, a logistic hail model has been developed by means of a multivariate analysis method. This statistical model is based on a combination of appropriate meteorological parameters (convective parameter, moisture content, etc.) and synoptic weather types. The output of the model is a new index that estimates the potential of the atmosphere for hailstorm development, referred to as potential hail index. Validations with independent data sets confirm the reliability of the model results. For Germany, the logistic hail model applied to reanalysis data over the past decades shows a markedly north-to-south gradient with most of the potential hail days occurring in the south. Applied to an ensemble of seven regional climate model simulations, it is found that the potential for hail events will increase in the future (2021–2050) compared to the past (1971–2000), but only statistically significant in the northwest and south of Germany.

1. Introduction

In Central Europe, severe hailstorms occurring almost exclusively during the summer half year may cause damage amounting to billions of USD. Examples include the severe hail event on 27 and 28 July 2013 in Germany with insured damage of 3.7 billion USD, representing the costliest insured loss event worldwide in 2013 [*Munich Re*, 2014]. Some insurance companies report a strong increase in hail damage over the past decades. Based on insured agricultural losses (1920–1999), *Schiesser* [2003], for example, found a substantial rise in the number of hail events in Switzerland between 1980 and 1994. *Kunz et al.* [2009] observed a rising trend both in the number of hail events and related losses from data of a building insurer in southwest Germany (Figure 1) over the past two decades. Using hailpad data from different areas of France, *Berthet et al.* [2011] found that whereas the number of hail events between 1989 and 2009 remained nearly constant, the intensity increased strongly. Given these few observations, the question arise to what extent the hail potential of the atmosphere already increased over the past decades and what changes can be expected for the future due to climate change.

Like all weather phenomena related to deep moist convection, hail streaks are spatially very limited. According to a study by *Changnon* [1970], 80% of all damage-causing hail streaks detected in the U.S. had a spatial extent of less than 40 km^2. Due to their local-scale extent and a lack of suitable observation systems in Germany, hail is not recorded accurately, homogeneously, and uniquely by existing archives. Most suitable for the identification and analysis of hail signals are weather radars, which have large areas under constant surveillance and offer a high temporal and spatial resolution [*Waldvogel et al.*, 1979; *Kunz and Puskeiler*, 2010]. However, at least in Germany, radar data are not yet available over long time periods. The same is true for data sets based on eyewitness reports like the European Severe Weather Database [*Dotzek et al.*, 2009] of the European Severe Storms Laboratory, which have a lack of spatial and temporal homogeneity. Insurance data are available over a longer period but lack of temporal homogeneity due to temporal changes in the vulnerability and the regulatory practice of the companies. Thus, no homogeneous long-term record of hail occurrence is available, which hampers statistical analyses and the identification of possible trends in the hail probability.

From a theoretical perspective, hail formation by accretion in cumulus clouds is most effective in environments with high liquid water content and large vertical velocity [*Pruppacher and Klett*, 1997]. These properties may be reliably reproduced by state-of-the-art cloud-resolving numerical weather prediction models but not

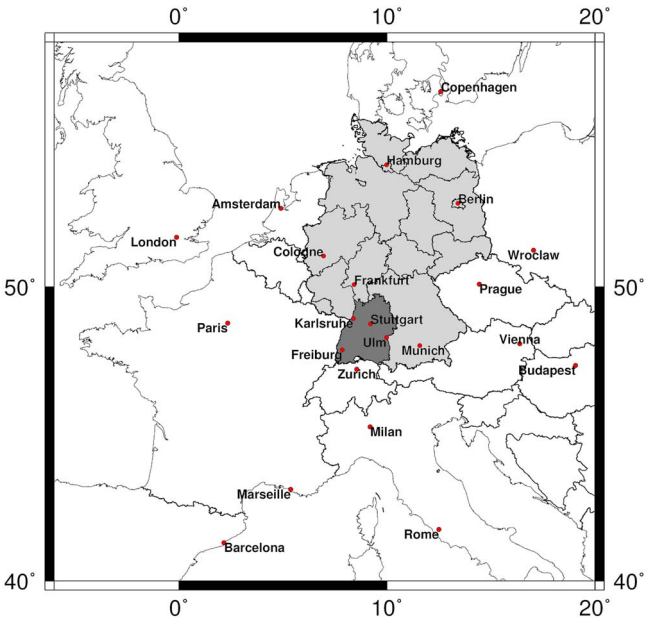

Figure 1. Part of Europe with the federal state of Baden-Württemberg (dark gray) in Germany (light gray).

by high-resolution regional climate models (RCMs). To overcome this limitation, convective indices derived from vertical temperature, moisture, and—in some cases—wind profiles or other meteorological parameters may serve as proxies for thermal stability (relevant for ascent), moisture content, and, thus, for hailstorm formation. Unlike direct observations, these proxy data exist over longer time periods with a sufficient homogeneity. If a relation between specific variables of the RCM and hail observations available for a limited region and a limited time period can be established, it might be possible to apply those relations to other regions and other periods where no direct observations are available. Changes in the proxies are also assumed to directly impact the probability and/or intensity of thunderstorms or hailstorms. Despite neglecting other important factors for hail formation such as appropriate aerosols (ice-forming nuclei) or lifetime of a storm, several studies have succeeded in establishing a relationship between those proxies and hail observations [e.g., *Huntrieser et al.*, 1997; *Groenemeijer and van Delden*, 2007; *Kunz*, 2007; *Sánchez et al.*, 2009; *Manzato*, 2012]. In particular, the convective available potential energy (CAPE) and the lifted index (LI) are suitable to predict deep moist convection [*Haklander and van Delden*, 2003; *Manzato*, 2003; *Mohr and Kunz*, 2013]. As shown, for example, by *Lee* [2002] or *Brooks et al.* [2003], convective parameters derived from general circulation models (GCMs) and RCMs can reproduce thermal stability of the atmosphere with sufficient accuracy. Reanalyses may reveal both the interannual variability and the days with observed instability. Furthermore, it is found that thunderstorms or hail events are more likely to occur (or not) during specific large-scale weather types [*Aran et al.*, 2010; *García-Ortega et al.*, 2011; *Kapsch et al.*, 2012], which can be reproduced from reanalyses or RCMs.

By using a multivariate approach to quantify the convective potential of the atmosphere as proposed in this study, several meteorological parameters relevant for the development of deep moist convection can be considered. According to *Applequist et al.* [2002], the logistic regression is a suitable statistical method to combine different parameters relevant for thunderstorm formation. This method has been successfully applied in different studies for binary diagnoses of thunderstorm or hail events [*Billet et al.*, 1997; *Sánchez et al.*, 2009; *Schmeits et al.*, 2005; *López et al.*, 2007].

This study aims at assessing the hail potential of the atmosphere in Germany including possible changes in past and future decades. For this assessment, a logistic hail model is developed, which combines several meteorological parameters obtained from RCMs. Describing the probability of hail occurrence is developed by means of logistic regression. The model is calibrated for a past period (1992–2000) using insurance loss data and a downscaled reanalysis run. It is validated with insurance data and a hail statistic for a different period. Afterward, the methods are transferred to an ensemble of high-resolution RCMs. Comparing the results for past and future time periods, expected changes in the hail potential are quantified. To estimate the reliability of the results, a miniensemble consisting of seven RCM runs is considered.

The paper is structured as follows: Section 2 gives a short overview of the used data sets and statistical methods. Section 3 is dedicated to the development and section 4 to the validation of the logistic hail model, whose results for the past and future are discussed in section 5. Finally, section 6 summarizes the results and gives some conclusions.

Table 1. Regional Climate Model Runs Used in This Study With Some Specifications

Model (Version)	Global Forcing	Horizontal Resolution	Emission Scenario	Run	Referred to as
CCLM–IMK (4.8)	ERA-40	0.065°	–	–	IMK40
CCLM–BTU (4.8)	ERA-Interim	0.11°	–	–	BTUInt
CCLM–IMK (4.8)	ECHAM5	0.065°	A1B	Run 1	IMKR1 C20/A1B
CCLM–IMK (4.8)	ECHAM5	0.065°	A1B	Run 2	IMKR2 C20/A1B
CCLM–IMK (4.8)	ECHAM5	0.065°	A1B	Run 3	IMKR3 C20/A1B
CCLM–CR (3.1)	ECHAM5	0.165°	A1B	Run 1	CRR1 C20/A1B
CCLM–CR (3.1)	ECHAM5	0.165°	A1B	Run 2	CRR2 C20/A1B
CCLM–CR (3.1)	ECHAM5	0.165°	B1	Run 1	CRR1 C20/B1
CCLM–CR (3.1)	ECHAM5	0.165°	B1	Run 2	CRR2 C20/B1

2. Data Sets and Methods

According to statistical analyses of radar and insurance loss data [*Kunz and Puskeiler*, 2010; *Mohr*, 2013], hailstorms in Germany occur most frequently from the afternoon until the early evening during the three summer months June, July, and August. Therefore, the investigations presented in this study refer to this quarter of the year. The used data sets and methods are briefly described below.

2.1. Regional Climate Model Data

The convective parameters and large-scale weather types considered in the logistic hail model are quantified from different high-resolution RCM simulations (see summary in Table 1). To estimate the spread and reliability of the results of future changes in the convective potential, we investigate the impact of the global forcing by different realizations and emission scenarios [*Nakićenović et al.*, 2000] and of different RCMs. Since some of these parameters require three-dimensional (3-D) meteorological fields, the number of available climate model runs for Germany is strongly limited. All our analyses are based on 12 UTC (around 12:40 local time), where the convective energy is highest, at least in the mean.

The model in climate mode, CCLM [*Rockel et al.*, 2008], is a nonhydrostatic RCM developed from the operational weather forecast model Consortium for Small-scale Modeling (COSMO) of the German Weather Service (DWD). Using CCLM version 4.8, different high-resolution climate runs were carried out by the Institute for Meteorology and Climate Research (IMK-TRO) at the Karlsruhe Institute of Technology (KIT) [*Berg et al.*, 2013; *Wagner et al.*, 2013]. The model data were calculated via double nesting of the model area (intermediate step of 0.440°) for Germany at a resolution of 0.065° (~7 km). For the control period 1971–2000 (C20) CCLM was driven both with ERA-40 reanalysis [*Uppala et al.*, 2005] from the European Centre for Medium-Range Weather Forecasts and with European Centre/Hamburg version 5 (ECHAM5)/MPI-OM runs 1–3 provided by the Max Planck Institute for Meteorology (MPI-M) in Hamburg, Germany [*Roeckner et al.*, 2003]. Estimates for the future are related to the period 2021–2050 (PRO). Since the results of the Intergovernmental Panel on Climate Change emission scenarios are still very similar until 2050, only the mean scenario A1B was used for the dynamical downscaling [*Schädler et al.*, 2012].

The CCLM-Consortium Runs (CCLM-CRs) [*Hollweg et al.*, 2008] are based on the earlier version CCLM 3.1 to simulate the climate for Europe. The runs were driven by ECHAM5/MPI-OM with two realizations ($R1 + R2$). For our study, we employed C20 and the two emission scenarios A1B and B1 with a horizontal resolution of 0.165° (~18 km; data stream 2).

A 20 year hindcast simulation of the period 1989–2008 for Europe was performed by the Chair of Environmental Meteorology at Brandenburg University of Technology (BTU) with CCLM version 4.8 and a horizontal resolution of 0.11° (~12 km). The simulation used a well-tested new standard configuration and was driven by interpolated six hourly data from ERA-Interim reanalysis [*Dee et al.*, 2011]. Soil moisture was initialized with values resulting from a previous 20 year test run with the same configuration in order to avoid spin-up effects due to a delayed soil adjustment during the first years of the simulation. The simulation is part of the EURO-CORDEX initiative, a coordinated regional climate downscaling experiment for Europe (see http://www.euro-cordex.net). The performance of the simulation has already been analyzed and compared with other

regional climate runs of the EURO-CORDEX model ensemble in several evaluation studies [*Vautard et al.*, 2013; *Kotlarski et al.*, 2014].

2.2. Meteorological Parameters

In the development process of the logistic hail model, we tested various convective indices and meteorological parameters (see Table A1) to obtain a combination that yields the highest prediction skill. As will be shown, most appropriate is the surface-based lifted index (SLI) [*Galway*, 1956]. The SLI is defined as the temperature difference between 500 hPa (T_{500}) and that of a parcel lifted from near-surface layers up to 500 hPa first dry adiabatically and, after reaching the lifting condensation level, moist adiabatically:

$$\mathrm{SLI} = T_{500} - T'_{S\rightarrow 500} \quad . \tag{1}$$

The lower (negative) the values of SLI, the more unstable the atmosphere. In a previous study, *Mohr and Kunz* [2013] have already shown that SLI among the various convective indices and parameters exhibits the best relation to hail damage days determined from insurance loss data.

2.3. Objective Weather Type Classification

In addition to the convective parameters, we considered also large-scale weather types based on the objective weather type classification of DWD [*Dittmann*, 1995; *Bissolli and Dittmann*, 2001]. This method separates among 40 different weather types (objective weather type, OWT) that are numerically quantified from weather forecast or climate models using the following scheme:

$$AA\mathrm{CI}_{950}\mathrm{CI}_{500}F \quad , \tag{2}$$

where *AA* indicates large-scale flow directions (NO = northeast, SO = southeast, SW = southwest, NW = northwest, and XX = no prevailing direction) determined from the *u* and *v* components of the wind vector in 700 hPa. CI_{950} and CI_{500} represent the cyclonality index (CI) in 950 and 500 hPa, respectively, determined from the relative vorticity ζ. Positive values indicate cyclonic (C), negative ones anticyclonic (A) flow. The parameter *F* considers the moisture content in the atmosphere through the precipitable water. If the value on a specific day is greater than the 10 day running average and long-term mean, the atmosphere is classified as wet (W), otherwise as dry (D). The identification of hail-related and hail-unrelated weather types is based on loss data provided by the Vereinigte Hagel for the period from 2001 to 2009 (see next paragraph).

Our analysis reveals that four weather types can be related to hail, whereas three are almost unrelated. Since the logistic model requires numerical values, the weather types are defined in a binary scheme:

$$\mathrm{OWT} = \begin{cases} 1 \quad , & \text{SWCAW, SWCCW, XXCAW, SWACW} \\ 0 \quad , & \text{all other OWTs} \\ -1 \quad , & \text{NWAAW, NWAAD, XXAAD} \end{cases} ,$$

Hail-related weather types, indicated by a numerical value of 1, include types with southwesterly flow directions, moist air masses, and cyclonic flow at at least one level. Hail-unrelated weather types, represented by −1, are characterized by anticyclonic flow at both levels and flow from northwest or without a defined direction. The weather types identified in our study approximately correspond with those obtained by *Kapsch et al.* [2012] for hail events in southern Germany and by *Bissolli et al.* [2007] for tornado occurrence in Germany.

2.4. Insurance Loss Data, Lightning Data, and Hail Events From Radar Data

For the calibration and validation of the logistic hail model, loss data provided by the building insurance company SV SparkassenVersicherung are used. Usually, buildings may become damaged by hailstones with a diameter exceeding 2–3 cm [*Gessler and Patty*, 2013]. Building insurance data are available for the period from 1992 to 2008 for the federal state of Baden-Württemberg (Figure 1, dark gray). The data set lists the number of loss reports, the resulting loss amounts, and contract information resolved into five-digit postal code zones. The losses have been inflation adjusted through 2010 and corrected with respect to the annual variability of the portfolio (for further information, see *Kunz and Puskeiler* [2010]). A day is defined as a hail day if at least 10 claims were settled on that day and if, moreover, the damage frequency (i.e., the ratio of damaged to insured buildings in percent) has amounted to at least 0.01% within the respective postal code zone.

All damage reports were additionally checked with lightning data of the European Cooperation for Lightning Detection network provided by Siemens. Only events in whose 40 km surroundings at least five flashes have been registered on a specific day have been taken into account. Overall, 67 days have been excluded from the insurance data set, most of them centered around a significant hail damage day. In the 9 years calibration period (1992–2000), 115 hail damage days (i.e., 14% of all days in the data set) have been considered in total. This corresponds to 12.8 days per year on average for the whole area of Baden-Württemberg. During the validation period (2001–2008), 146 hail damage days (20%) have been recorded (18.3 days per year).

For the identification of hail-related and hail-unrelated weather types (see previous paragraph), we used loss data from the Vereinigte Hagelversicherung, which is a special insurer for agricultural products. The data set covers the whole area of Germany and only indicates whether there was hail damage or not in regions comparable to five-digit postal codes zones.

Another validation is performed for hail signals derived by *Puskeiler* [2013] from a combination of 3-D radar data of the DWD radar network, lightnings, and insurance loss data. The hail statistics are available for the summer half year (April–September) between 2005 and 2011. The hail criterion applied to radar data is an adjusted version of the Waldvogel method [*Waldvogel et al.*, 1979]. The results show a high correlation with the insurance data described above (e.g., Heidke Skill Score (HSS) ~0.70). For more details, the reader is referred to the study of *Puskeiler* [2013]. Here we used the hail statistics for the period 2005 to 2008 to determine whether a specific day was a hail day or not. Overall, hail signals in the radar data were detected on 250 days, that is, on 68% of all days within the time frame considered (summer months).

2.5. Logistic Regression

Using a multiple logistic model, the occurrence probability p of an event is investigated as a function of different meteorological factors $\{x_1, x_2, \ldots, x_n\}$ as independent variables [*Hosmer and Lemeshow*, 2000]. As a rule, a dichotomous scheme (e.g., hail YES/NO) is defined as a dependent variable y. Hence, the occurrence probability is given by

$$y = p(x) = \frac{1}{1 + e^{-g(x)}} \qquad \text{with } 0 \le p(x) \le 1 \quad , \tag{3}$$

with the model based on the linear regression:

$$g(x) = \beta_0 + \beta_1 x_1 + \beta_2 x_2 + \ldots + \beta_n x_n \quad . \tag{4}$$

The regression parameters β_n are derived by applying the maximum-likelihood method to maximize the probability. This means that the coefficients are determined through an iterative method, which ensures that the estimated variables are as close as possible to the original data.

When evaluating the quality of the logistic regression model, one differentiates between the assessment of the quality of the overall model and that of the individual independent variables [*Backhaus et al.*, 2011]. The overall model LL_V is that which includes stepwise all independent variables. The significance of the overall model is checked using the likelihood ratio test (LRT) which compares the log likelihood of the overall model LL_V with that of the null model LL_0 (i.e., $\beta_1 = \beta_2 = \ldots = \beta_N = 0$):

$$\mathrm{LRT} = -2\frac{\mathrm{LL}_0}{\mathrm{LL}_V} = +2(\mathrm{LL}_V - \mathrm{LL}_0) \quad . \tag{5}$$

Note that the terms in the ratio are logarithmic, thus allowing the expansion on the far right. If LRT is significantly different from zero, the model with its independent variables has a significant explanatory power (mostly $\alpha = 0.05$).

Applying the likelihood quotient test (LQT), it is checked stepwise forward whether another independent variable can improve the model approach used so far. Similarly, as in the likelihood ratio test, the likelihood of the overall model LL_V is compared with that of a model reduced by the influence of one variable (or several variables) LL_R and with the corresponding regression coefficient set to zero [*Hosmer and Lemeshow*, 2000]:

$$\mathrm{LQT} = +2(\mathrm{LL}_R - \mathrm{LL}_V) \quad . \tag{6}$$

Due to the exponential relation between the independent and the dependent variables, the effect of the individual regression coefficients β_n on the probability p cannot be determined directly. Using the effect

coefficient ec allows to estimate which of the variables x_n has the strongest impact on the occurrence probability y of a binary event [*Backhaus et al.*, 2011]. The strength of the respective effect is measured by the standard deviation of the independent variable $\sigma(x_n)$. Hence, the standardized effect coefficients are quantified by

$$\mathrm{ec}_n = e^{\beta_n \cdot \sigma(x_n)} \quad . \tag{7}$$

Since in the case of regression coefficients with $\beta_n < 0$, the effect coefficient is $\mathrm{ec}_n < 1$, the reciprocal value of the latter must be considered for comparisons with the results of other variables. This is necessary in case of a negative correlation between variable x_n and the event, for example, between SLI and hail (for further details, see *Mohr*, [2013]).

3. Design of the Logistic Hail Model

The logistic hail model (equation (3)) is determined separately at each grid point (33 × 38) of the regionalized reanalysis run (IMK40) for the federal state of Baden-Württemberg. It is calibrated against insured hail damage within a detection radius of 100 km (1992–2000). This radius provides a good correlation between convective parameters and convective events as, for example, suggested by *Haklander and van Delden* [2003]. The different regression coefficients β_n (equation (4)) are estimated through a quantitative comparison between the meteorological variables x_n and the observations. The probability p_{hail} of the occurrence of hail can be calculated afterward by using the logistic model obtained.

Being the variable with the highest prediction skill for hail according to *Mohr and Kunz* [2013], SLI is the first parameter to be integrated into the model. Using a stepwise forward method, the next new variable x_n is determined by the LQT (equation (6)). Only those variables are further considered that yield an improvement of the logistic model in terms of a positive result of LQT and higher skill scores based on categorical verification. For the latter, different accuracy measures such as the probability of detection (POD) or the false alarm rate (FAR) and skill scores such as HSS or Peirce skill score (PSS, also known as the true skill statistic) are quantified between the results of the logistic model and the hail damage days according to the insurance data [*Wilks*, 2006]. After that, the explanatory power of the overall model is subsequently checked using the LRT (equation (5)).

A total of 36 different convective and meteorological parameters were tested as variables x_n (see Table A1). According to the stepwise forward method, most suitable for the logistic hail model are the following four parameters: (1) surface-based lifted index at 12 UTC (SLI), (2) minimum near-surface temperature (T_{min}), (3) near-surface temperature (T_{2m}) at 12 UTC, and (4) hail-related and hail-unrelated objective weather types (OWTs).

These parameters reflect the atmospheric stability, advection of specific air masses, and near-surface conditions in the morning and early afternoon, respectively. T_{min} is a measure for the wet-bulb potential temperature θ_w in the afternoon and a reasonable indicator for the conditions prevailing in the morning in the boundary layer [*Willemse*, 1995; *Dessens*, 1995; *Sánchez et al.*, 1998, 2008]. Higher temperature in this layer at night causes less nocturnal inversion at low levels due to long-wave radiation and may lead to higher moisture contents. In this sense, T_{min} is also relevant for the formation of convection in the early afternoon. This conclusion is confirmed by the fact that consideration of T_{min} in the logistic model becomes redundant if other parameters related to near-surface moisture are used, for example, TQV, r_{2m}, $T_{d,2m}$, or $T_{d,850}$. All these parameters could be used in principle instead of T_{min}.

In many studies, $p_{\mathrm{hail}} \geq 0.5$ defines the common threshold value as criterion for the occurrence of an event [*Hosmer and Lemeshow*, 2000; *Sánchez et al.*, 1998, 2009; *López et al.*, 2007]. However, upon closer examination, we found that the number of events would be underestimated for this threshold. The receiver operating characteristic (ROC)—or simply ROC curve—can provide an objective way to determine the dichotomizing threshold [*Jolliffe and Stephenson*, 2012]. The ROC curve is a graph of the POD against the probability of false detection (POFD) as the decision threshold changes. Values that are close to the diagonal (POD = POFD) indicate random processes (black line in Figure 2). Perfect discrimination is represented above the diagonal with values showing the highest distance H to the diagonal. This applies also when the PSS (POD − POFD) is maximized [*Manzato*, 2007]. In Figure 2, all ROC curves for a selection of various grid points show a good discrimination. An optimum threshold p_{hail} varies between 0.1 and 0.2 depending on the respective grid point (light gray). The closely positioned curves support the use of a constant value for p_{hail}. A value of $p_{\mathrm{hail}} = 0.2$, for example, is equivalent to PSS = 0.53. All further analyses are based on a threshold of $p_{\mathrm{hail}} \geq 0.2$.

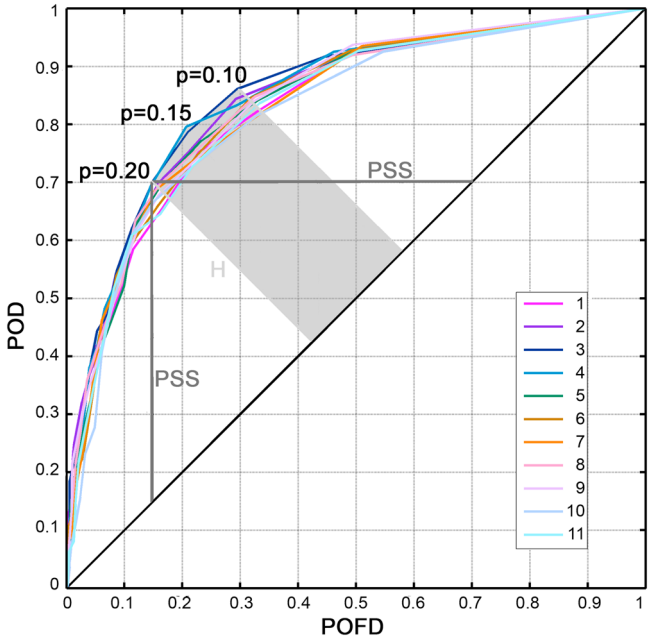

Figure 2. The ROC curve for varying thresholds p_{hail}. The light gray shaded area indicates the best values of the threshold depending on the logistic hail model for different grid points (1–11; see Figure 3). See full text for more details.

Following the ideas described above, the linear regression model (equation (4)) that gives the best results is defined by

$$g_{\text{hail}} = \beta_0 + \beta_1 \cdot \text{SLI} + \beta_2 \cdot T_{\min} + \beta_3 \cdot T_{2m} + \beta_4 \cdot \text{OWT} \quad , \tag{8}$$

$$\text{where } p_{\text{hail}} = \begin{cases} < 0.2 & , \text{ hail: NO} \\ \geq 0.2 & , \text{ hail: YES} \end{cases} .$$

In the following, the logistic hail model described by equation (8) is abbreviated as LHM. The index obtained by the LHM, referred to as potential hail index (PHI), quantifies the number of days on which hail is likely to occur.

Table 2 show the results of the categorical verification for the stepwise forward method of the logistic hail model by adding new parameters. A direct comparison between SLI and hail events already yields a high HSS of 0.36. Adding a new parameter, the skill of the model is enhanced step by step—particularly for $T_{\min}$—up to a maximum value of HSS = 0.43. Note that the POD increases more than twice (0.32 for the direct comparison and 0.68 for the LHM), whereas the FAR almost remains the same (0.57 and 0.6). For the last step (T_{2m}), the improvement is only marginal. However, including T_{2m} gives a higher HSS for more grid points or LHMs.

Since at each grid point an individual logistic hail model is obtained with different regression coefficients, the question arises as to which of the 33×38 model configurations is best suited for determining the hail potential of the atmosphere representative for a larger domain. The quality of each individual logistic models can be checked among each other by means of the pseudo-coefficient of determination after McKelvey and Zavoina (MKZ-R^2) [*McKelvey and Zavoina*, 1975]. The MKZ-R^2 is based on the explained variance:

$$\text{MKZ-}R^2 = \frac{\sum_{i=1}^{N} \left(\hat{y}_i^* - \hat{\bar{y}}_i^*\right)^2}{\sum_{i=1}^{N} \left(\hat{y}_i^* - \hat{\bar{y}}_i^*\right)^2 + N} \quad \text{, where} \quad \hat{\bar{y}}_i^* = \frac{1}{N} \sum_{i=1}^{N} \hat{y}_i^* \tag{9}$$

Table 2. Accuracy Measures (POD and FAR) and Skill Scores (HSS and PSS) Based on Categorical Verification of Predicted Hailstorms Verified With Hail Damage Days According to Insurance Data (1992–2000)[a]

	$\text{HSS}_{98\%}$	HSS_{mean}	$\text{PSS}_{98\%}$	POD_{mean}	FAR_{mean}
SLI (direct)	0.36	0.28	0.36	0.32	0.57
SLI (by logistic regression)	0.36	0.31	0.47	0.58	0.66
SLI + OWT	0.38	0.34	0.49	0.61	0.64
SLI + OWT + $T_{\min}$	0.42	0.38	0.55	0.67	0.61
SLI + OWT + $T_{\min}$ + T_{2m}	0.43	0.39	0.56	0.68	0.60

[a]The first row indicates the verification results for SLI (< −3.6 K) without considering the logistic model. The other rows depend on the logistic regression model with changing number of parameters x_n. Mean (98%) stands for an average value (98% percentile) of an area with 15 × 16 (= 240) grid points in the center of the investigated field.

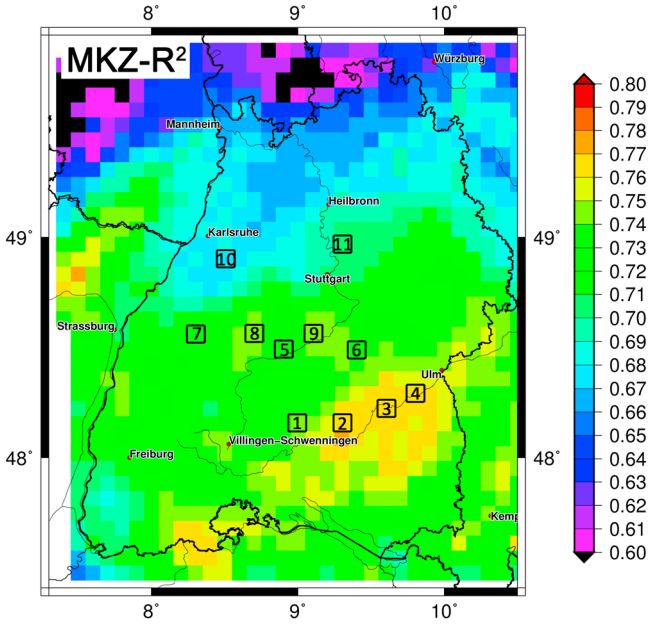

Figure 3. Pseudo-coefficients of determination after MKZ-R^2 (values ≥ 0.7 indicate a good explanatory power) for each of the 33×38 model configuration between IMK40 and insurance data (1992–2000) to compare the different model quality. The numbers indicate the grid points where the logistic hail models will be applied afterward.

and N is the sample size. High values of MKZ-$R^2 \geq 0.7$, which are indicative of a good explanatory power of the LHM, are found particularly in the center of the investigation area with a maximum southwest of the city of Ulm (Figure 3). To account for the LHM-dependent uncertainty of the results, we created for the following analyses an ensemble consisting of 11 different models. Sensitivity analyses, where the size of this ensemble was varied, are described in section 5.1. The grid points with the respective LHMs are selected so that both models with the highest (e.g., 2–4) and lower (e.g., 10 and 11) skills are considered to describe the variability achieved. Table 3 (top) lists the values of the individual logistic regression coefficients β_n as a function of the used variable x_n for the 11 LHMs. It is apparent that the β_n values of the individual models do not exhibit an excessive spread. This proves that the individual LHMs do not differ too much from one grid point to another. From this, one can conclude that differences in the LHMs that may be caused by orographic or climatological influences are rather small.

To exclude multicollinearities, the correlations between the four parameters described above are analyzed by means of the variance inflation factor

$$\mathrm{VIF}_n = \frac{1}{1 - r_n^2} \quad , \tag{10}$$

where r_n^2 is the coefficient of determination between two independent variables x_n [*Götze et al.*, 2002]. The presence of multicollinearity could result in unstable regression coefficients, which means that they change strongly when a variable x_n is added or removed. This may lead to a falsification of the results. The larger the variance inflation factor is, the more probable is a correlation between the parameters. However, a general accepted convention for multicollinearity does not exist. In different studies the threshold for multicollinearity differs between 4 and 10 [e.g., *O'Brien*, 2007]. If the inflation factor is determined for different parameters x_n

Table 3. Logistic Regression Coefficients β_n (Top) and Related Effect Coefficients ec_n (Bottom) for the LHMs at Points 1 to 11 (Subscript; see Figure 3), Based on IMK40 and Hail Damage Days According to Insurance Data Between 1992 and 2000

x	LHM_1	LHM_2	LHM_3	LHM_4	LHM_5	LHM_6	LHM_7	LHM_8	LHM_9	LHM_{10}	LHM_{11}
	$\beta_0 = -1.60$	−2.16	−2.53	−2.73	−2.54	−2.06	−1.72	−2.22	−2.49	−3.15	−3.49
SLI	$\beta_1 = -0.36$	−0.37	−0.36	−0.34	−0.31	−0.32	−0.32	−0.32	−0.32	−0.21	−0.25
$T_{\min}$	$\beta_2 = 0.32$	0.31	0.32	0.29	0.29	0.30	0.36	0.32	0.29	0.29	0.28
T_{2m}	$\beta_3 = -0.24$	−0.21	−0.20	−0.18	−0.17	−0.21	−0.27	−0.21	−0.18	−0.16	−0.13
OWT	$\beta_4 = 0.64$	0.64	0.67	0.65	0.63	0.59	0.47	0.63	0.62	0.58	0.58

x	ec_1	ec_2	ec_3	ec_4	ec_5	ec_6	ec_7	ec_8	ec_9	ec_{10}	ec_{11}	Mean
SLI	4.3	4.7	4.7	4.4	3.7	4.0	3.9	3.9	4.0	2.6	2.9	**3.9**
$T_{\min}$	3.1	2.9	2.9	2.7	2.7	3.0	3.8	3.0	2.7	2.9	2.5	**2.9**
T_{2m}	3.4	2.8	2.7	2.4	2.4	3.0	4.0	2.8	2.4	2.2	1.9	**2.7**
OWT	1.5	1.5	1.5	1.5	1.5	1.4	1.3	1.5	1.5	1.4	1.4	**1.5**

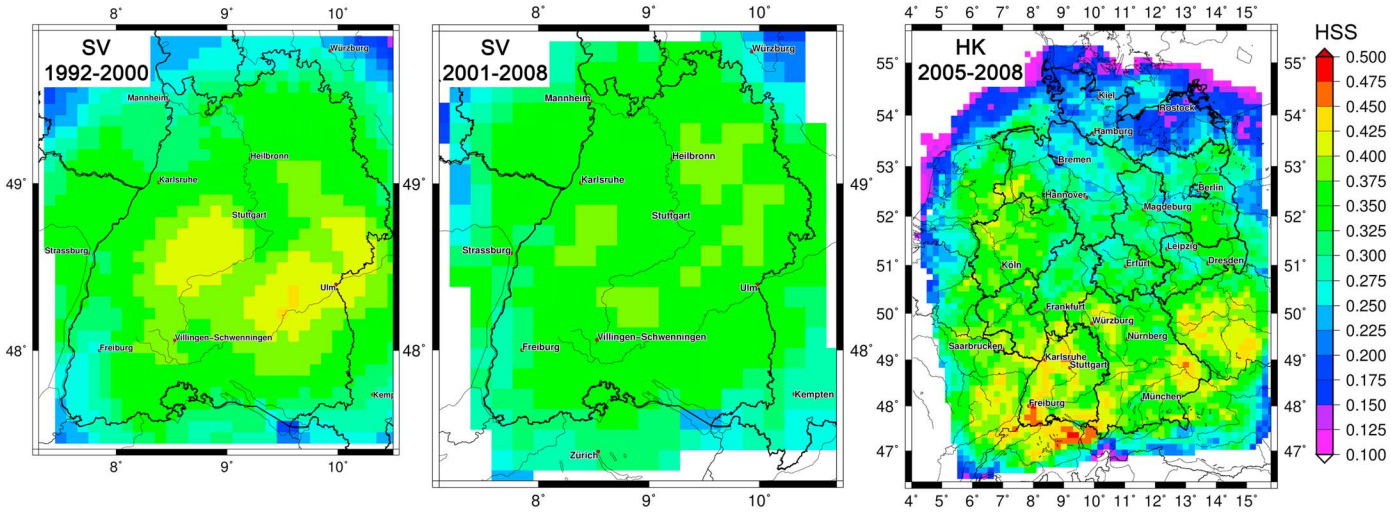

Figure 4. Verification of the developed 11 logistic hail models with the Heidke Skill Score (HSS) between (left) IMK40 and insurance data (1992–2000), (middle) BTUInt and insurance data (2001–2008), and (right) BTUInt and hail signals based on radar data (2005–2008).

in the LHMs, only values below 4 result. Furthermore, the correlation coefficient r between SLI and T_{2m} only shows a slight correlation with values between 0.45 and 0.52, depending on the respective grid point.

In addition, the question arises as to which of the used variables has the greatest effect on p_{hail}. Applying equation (7), the effect coefficient ec_n is calculated for each independent variable x_n of the 11 LHMs (Table 3, bottom). The larger the values, the greater the effect strength of the variables with respect to the result of the relevant logistic model. If the value corresponds to 1, the variable has no effect on the result. According to Table 3 (bottom), SLI has the greatest influence on the probability in almost all individual models (LHM_1 – LHM_{11}). Only in the case of LHM_{10} the effect of T_{min} is greater than that of SLI. Having values in a range between 2.7 and 2.9 averaged over all models, T_{min} and T_{2m} show similar effects. It becomes clear that both, SLI and T_{2m}, have a significant contribution to the LHMs despite a small correlation of about 0.5. Also, the results of a LHM with or without T_{2m} differ considerably. Therefore, both parameters have to be included. Although being the smallest of all, the contribution of the OWT still is significant. As already found in the case of the logistic regression coefficients β_n, the difference between the models is not very pronounced.

4. Validation of the Logistic Hail Model

To further assess the reliability of the logistic model approach, an additional validation is performed using two independent data sets. For this, we quantified the LHM ensemble as described above from the recently released BTUInt hindcast model runs. For the verification, we applied the hail statistics obtained from a multicriteria approach including radar, loss, and lightning data (see section 2).

Since the individual regression coefficients β_n of the LHMs have been specifically adapted to the climatological conditions prevailing in IMK40, a bias correction has to be applied prior to the statistical analysis using BTUInt. Without bias correction, the variability of PHI among the different RCMs would be too large. Because the BTU-Int simulations overestimate the summer temperatures compared to IMK40, the bias correction is performed for SLI, T_{min}, and T_{2m}. This correction is based on the frequency distributions of the respective parameters for the whole area and periods. For SLI, the bias is +2.0 K; for T_{min} it is −0.7 K and for T_{2m} −2 K.

After applying the bias correction, the results of the PHI ensemble quantified from BTUInt hindcasts are compared at first with building insurance data in Baden-Württemberg (2001–2008; Figure 4, middle). The values and spatial distribution of HSS (mean of the 11 models) are almost similar to that obtained from IMK40 (1992–2000; Figure 4, left). The highest values above 0.35 are found in the center of the investigation area. The decrease toward the boundaries of the domain is due to the fact that most of the hail damage events (≈95%) are recorded in the central area by considering a detection radius of 100 km (see section 3). Overall, PHI derived from IMK40 performs slightly better compared to BTUInt (see Table 4). This may be related to the fact that the LHMs are calibrated for the same period of IMK40. Further, the values of HSS depend on the

Table 4. Accuracy Measures (POD and FAR) and Skill Scores (HSS and PSS) Based on Categorical Verification of Predicted Hailstorms per LHM Verified for IMK40/BTUInt and Hail Damage Days (Baden-Württemberg)/Hail Signals From Radar Data (All of Germany)[a]

	$HSS_{98\%}$	HSS_{mean}	$PSS_{98\%}$	POD_{mean}	FAR_{mean}
IMK40 ↔ insurance (1992–2000), 15 × 16	0.42	0.39	0.55	0.65	0.60
BTUInt ↔ insurance (2001–2008), 15 × 16	0.39	0.36	0.48	0.64	0.58
BTUInt ↔ radar (2005–2008), Germany	0.43	0.33	0.42	0.44	0.47
BTUInt ↔ radar (2005–2008), South Germany	0.44	0.37	0.44	0.49	0.41
BTUInt ↔ radar (2005–2008), North Germany	0.39	0.29	0.37	0.40	0.53

[a]15×16 means 240 grid points in the center of Baden-Württemberg. South (North) Germany means only grid points below (above) 51°N. Mean (98%) stands for an average value (98% percentile) of the respective investigated area.

climatological event frequency [*Hamill and Juras*, 2006]. Tests with varying time periods, however, show that these effects are not very high and normally smaller than 0.025 HSS. Most important in this comparison, however, is the fact that the evaluation results of IMK40 and BTUInt are very similar, despite the different periods considered (1992–2000 versus 2001–2008). This is a further indication that this approach is sufficiently robust.

Validated with hail days from the radar composite for Germany between 2005 and 2008, the results of BTUInt show higher HSS values up to 0.49 compared to the evaluation with insurance data (recall that IMK40 is not available after 2000). The higher HSS may be due to the complete coverage of the investigation area of the radar data. Regions with high HSS values (>0.4) can be observed in parts of Southern Germany and North Rhine-Westphalia. Overall, the LHMs fit better in southern Germany ($HSS_{mean} = 0.37$) compared to the north ($HSS_{mean} = 0.29$; see Table 4). Particularly, near the coast of the Baltic Sea the values are low. This must be kept in mind when the LHMs are quantified from the future RCM ensemble for Germany (section 5.2). The reasons for these differences are probably the different climatologies of static stability or properties in the near-surface layers in the north. Most important, however, is the finding that the LHM is transferable to a larger region, in this case the whole area of Germany (particularly south of 52°N). These results shall be discussed in the next section.

5. Assessment of Hail Potential

In this section, we apply the LHM ensemble approach to two different 30 year time frames: the one is the whole C20 period (1971–2000) using IMK40 downscaled reanalysis and the other is the PRO period (2021–2050) using a miniensemble of seven RCMs.

5.1. Hail Potential in the Past

The median of PHI quantified from the 11 LHMs from IMK40 during C20 (Figure 5, left) shows a markedly north-to-south gradient with highest values in the south. Whereas hail is expected to occur on 8 to 14 days a year north of line of approximately 50°N, southern Germany exhibits an annual average of 17.4 ± 3.3 potential hail days. Highest PHI values (22 to 28 days) are found in the Rhine Valley (north of Freiburg) and southeast of Munich at the border to Austria. Over the Alps in the very south, the occurrence probability is smallest, mainly due to the lower near-surface temperatures in elevated areas. This also applies to the low mountain ranges, where the PHI is generally smaller compared to the lowlands. Averaged over the entire area under investigation, the mean annual PHI is 14.9 ± 3.4 days. It should be noted that the results over Lake Constance (region with the maximum in Figure 5) are highly uncertain because a lake model was not included, yielding unrealistic sea surface temperatures [*Mironov et al.*, 2010].

Compared to the median, the overall standard deviation of PHI (Figure 5, right) is relatively small and, naturally, related to the form. In areas where the values of PHI are high, the standard deviation is enhanced as well. The variation coefficient (<0.2), which is standard deviation normalized by the mean, does not show any remarkable or systematic spatial variability (not shown).

The step-by-step development of the LHM reveals that the climatology of the respective variables integrated into the model substantially affects the spatial distribution of the PHI results. Hence, the high number of potential hail days in the Rhine Valley and in the northern foothills of the Alps is related to a lower thermal

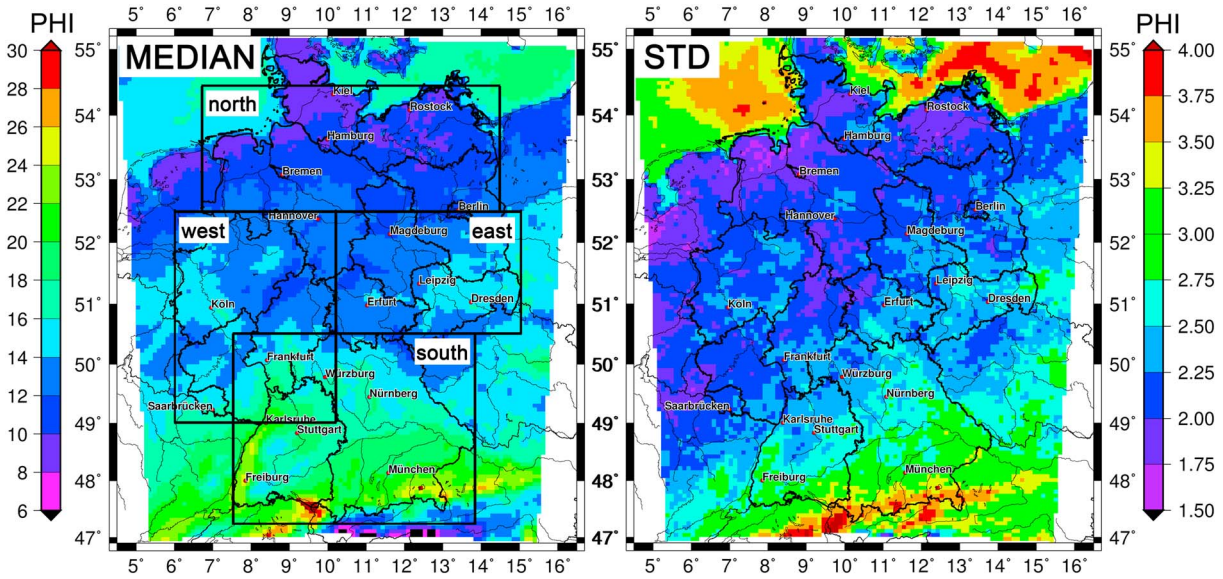

Figure 5. (left) Median and (right) standard deviation (STD) for the annual potential hail index (PHI) derived from the 11 LHMs (IMK40, 1971–2000). In Figure 5 (left), the mean values of the subdivided areas are north 11.9 ± 2.2 days, west 13.7 ± 1.5 days, east 13.4 ± 1.1 days, and south 17.4 ± 3.3 days.

stability and a higher moisture content in those areas. In contrast, thermal stability in the north is higher due to the prevailing colder and drier conditions.

The overall spatial distribution of PHI is in good accordance to the north-to-south gradient shown by the few available hail climatologies [e.g., *Hand and Cappelluti*, 2011; *Puskeiler*, 2013; *Punge et al.*, 2014]. For example, the high PHI values prevailing in southern Bavaria and in the center of Baden-Württemberg or the very low values offshore are also found in the spatial pattern of lightning density or radar reflectivity [*Kunz and Puskeiler*, 2010; *Puskeiler*, 2013]. However, the LHM cannot match several features of these studies that occur especially on the local scale, such as the location of the maxima in Baden-Württemberg or Bavaria. These discrepancies can be attributed to the limited parameter space that is incorporated in the LHM. In particular, over complex terrain, convergence zones due to thermally direct circulation or flow deviation around obstacles are most decisive for the location of convective initiation [*Barthlott et al.*, 2011]. For example, *Knight and Knight* [2003] and *Kunz and Puskeiler* [2010] have shown that hail can often be observed on the lee side of mountains. Semi-idealized COSMO simulations revealed that the flow around the mountains at low Froude numbers in combination with gravity waves intensifies horizontal flow convergence on the lee side, which in turn may trigger or intensify thunderstorms (not yet published). The LHM, however, relies on parameters which only describe the preconvective environment and which do not consider mechanisms and processes relevant for convective initiation. These trigger mechanisms, however, cannot be incorporated in the model since convergence zones are not well captured by the RCMs. As already mentioned, the LHM only quantifies the potential for hail to occur and the results have to be interpreted accordingly. Thus, the PHI cannot be related to single grid points; rather, it represents a larger area around that point.

To further assess the robustness of the methods and results, various additional analyses were carried out by changing the following points: (i) months considered (May to July instead of June to August); (ii) radius around the grid points where hail events are considered (50 instead of 100 km); (iii) damage frequency in the insurance data for the definition of a hail day (0.1 and 0.5 instead of 0.01%); (iv) size of the ensemble (21 and 31 instead of 11 LHMs); (v) threshold values for the probability of hail (0.15, 0.3, 0.4, and 0.5 instead 0.2); and (vi) meteorological parameters in the hail model (e.g., CAPE, TQV, and TT). Overall, the results obtained using the modified model are mostly similar to the results discussed above. For example, the results of the PHI for an ensemble consisting of 31 LHMs display very small deviations (ΔPHI $<$ 0.5 days) on most of the grid points (75%; not shown). Only a few areas show a difference of up to one hail day per year compared to the original LHM. These changes are due to the fact that as further grid points are selected, more LHMs with less explanatory power that underestimate the PHI are incorporated in the ensemble. Only changes in the hail probability p_{hail} have a larger impact on the results. The spatial pattern obtained for this modification, however, shows only marginal differences.

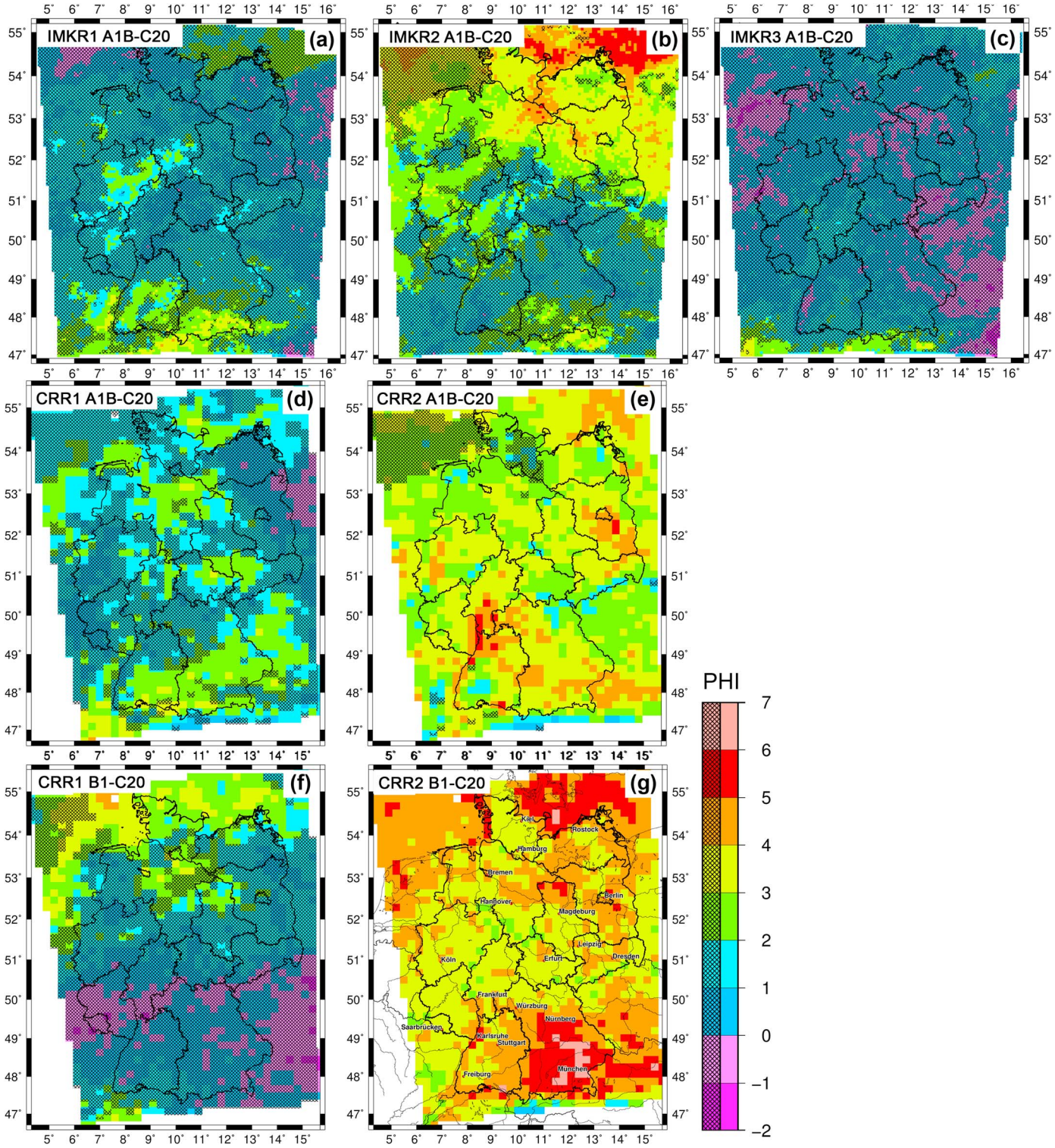

Figure 6. Difference of average potential hail index (PHI) for the (a–c) CCLM-IMK and (d–g) CCLM-CR runs between future and past (2021–2050 compared with 1971–2000). Trends with significance below 95% are cross hatched. Note that a PHI decrease is statistically significant only at a few grid points (1%).

Finally, linear trend analyses of the PHI reveal for most areas in Germany an increase in the hail potential (IMK40, 1971–2000; not shown). However, considering the statistical significance of these linear trends, it turned out that most of the grid points have a level of significance below 95%. This reduced significance was already found in trend analyses of single convective parameters from the same RCM run [*Mohr*, 2013].

Table 5. Spatial Means and Standard Deviations of the Climatology (C20, PRO) of the Mean Potential Hail Index (PHI) and Difference Between PRO and C20 for the CCLM-IMK and CCLM-CR Runs as Well as Normalized by C20

Model Run	Climatology (days)	Absolute Change (days)	Relative Change (%)
IMK40	14.9 ± 3.4	–	–
IMKR1 C20	13.8 ± 2.7	–	–
IMKR2 C20	13.5 ± 2.9	–	–
IMKR3 C20	13.6 ± 2.9	–	–
IMKR1 A1B	15.1 ± 2.8	1.4 ± 0.8	10.1
IMKR2 A1B	16.0 ± 3.0	2.5 ± 1.1	19.9
IMKR3 A1B	14.2 ± 3.0	0.6 ± 0.7	4.4
CRR1 C20	13.2 ± 4.7	–	–
CRR2 C20	12.7 ± 4.3	–	–
CRR1 A1B	14.8 ± 4.8	1.6 ± 0.7	15.3
CRR2 A1B	15.9 ± 4.7	3.2 ± 0.8	29.7
CRR1 B1	14.4 ± 4.3	1.2 ± 1.2	12.9
CRR2 B1	16.9 ± 4.5	4.1 ± 0.8	40.6

Reasons are the high annual variability of the PHI and the convective parameter, respectively. Across Europe, increases and decreases of hail events are found in the scarce literature. Whereas, for example, in North Italy, *Giaiotti et al.* [2003] found no upward trend in the number of hail days (1988–2001), *Eccel et al.* [2012] report on a slight decrease in the number of hail days estimated from hailpad data (1975–2009). In France, *Berthet et al.* [2011] found in hailpad analyses a strong increase in hail intensity of 70% between 1989 and 2009, while the frequency of hail events did not change significantly.

5.2. Changes of the Hail Potential in the Future

In the last step, the LHM is applied to a miniensemble of different RCM runs (see Table 1) with the objective to quantify possible changes in the hail potential in the future. By doing so, we assume that the four parameters selected for the LHM (SLI, T_{2m}, T_{min}, and OWT) during the training period are also appropriate to describe the convective potential in the future. For the consortial runs (CCLM-CRs), a bias correction for SLI and T_{2m} was applied as described in section 4. For SLI, the bias is +2.5 K; for T_{2m}, it varies between ±5°C (applied only for temperatures >17.5°C) (for details, it is referred to *Mohr* [2013]).

Overall, the individual model runs show significant differences in the changes of PHI between the projection period PRO (2021–2050) and C20 (Figure 6 and Table 5). The largest variability is found for the different realizations of ECHAM5, especially for run 3 (Figure 6c) compared to run 1 or run 2. The specific version of the RCM is of minor importance as the patterns between the IMK and consortial runs driven by ECHAM5 runs 1 (Figures 6a and 6d) and 2 (Figures 6b and 6e) are comparable. The influence of the underlying emission scenario remains unclear: whereas the spatial distribution of PHI substantially changes between A1B and B1 for CCLM-CR run 1 (Figures 6d and 6f), it is almost the same for CCLM-CR run 2—only with higher values in B1 compared to A1B (Figures 6e and 6g). One can conclude that most of the uncertainty in the change signals is caused by internal climate variability as expressed by the different realizations of the driving GCM. This finding is in agreement with other studies, for example, that of *Hawkins and Sutton* [2011] or *Wagner et al.* [2013], who show that for near-future precipitation projections internal variability uncertainty is largest, whereas scenario uncertainty is almost negligible.

Concerning the magnitude and sign of the change signals, the majority of the seven RCM runs shows an increase in the median of PHI. Almost all model runs project the largest increase in PHI (2–6 days) at the southern border region between Germany and Switzerland and over the northern foothills of the German Alps. A total of more than 81% of all grid points of each run show an increase of PHI. For the RCMs driven by ECHAM5 run 2, this applies even to almost all grid points. Averaged over the entire area, an average PHI increase of 20–41% is expected for these three simulations. The greatest positive changes of up to 41% ($+4.1 \pm 0.8$ days) are expected for the consortium run CRR2 B1 with the highest values in Bavaria (Figure 6g). Only the two runs IMKR3 A1B (Figure 6c) and CRR1 B1 (Figure 6f) project a decrease in PHI for around 20% of the area. Whereas this decrease is mainly restricted to the southern parts in CRR1 B1, it is more or less evenly distributed in IMKR3 A1B.

The overall positive PHI trend expected for the future from the RCM ensemble can be ascribed to two effects: a tendency toward a higher probability for large-scale weather types that favor hailstorm development [*Kapsch et al.*, 2012] and an increase in the near-surface temperature, both in the morning and at 12 UTC. Following the

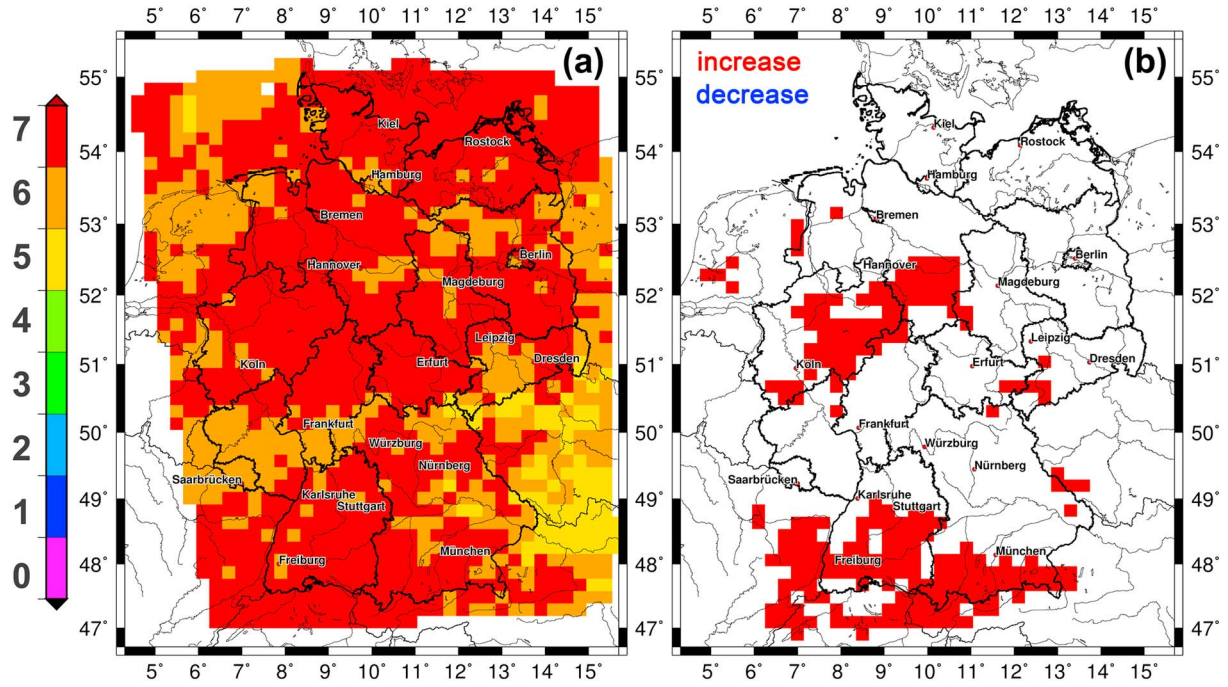

Figure 7. Overview of changes in the potential hail index (PHI) between 2021–2050 and 1971–2000 represented by an ensemble of seven climate simulations: (a) number of runs showing an increase and (b) changes when at least five of the seven runs show a significant increase according to the Wilcoxon rank-sum test.

Clausius-Clapeyron equation, the latter causes an increase in the moisture content and, thus, in the convective energy. The connection between water vapor content in the boundary layer and deep moist convection has been already observed by *Trapp et al.* [2007] for the U.S. On the other hand, both the lapse rate (e.g., surface/500 hPa and 850/500 hPa) and the SLI suggest a slight increase in atmospheric stability. These changes, however, have a less impact on the overall PHI result.

To estimate the statistical significance of the changes in the PHI medians, the nonparametric Wilcoxon rank-sum test ($\alpha = 95\%$, two sided) was applied [*Wilks*, 2006]. Changes that are not significant are cross hatched in Figure 6. It is evident that all negative changes are not significant. By contrast, the runs driven by ECHAM5 R2 indicate significant changes for most of the grid points.

For better illustration, the results of all RCM runs are summarized by counting at each grid point the number of climate simulations showing a PHI increase in PRO compared to C20 (Figure 7a). It becomes evident that for almost all grid points, at least five of the seven RCMs project an increase in the hail potential in the future. These changes are statistically significant on the 95% level in at least five of the seven model runs in the region between Germany and Switzerland or Austria, respectively, and for an area northeast of the city of Cologne (Figure 7b).

6. Discussion and Conclusion

In this study, we have developed and applied a logistic hail model (LHM) for the quantification of the hail potential over the past (1971–2000) and future (2021–2050) decades. Different convective parameters and large-scale weather patterns were derived from high-resolution climate simulations driven by ERA-40 and ERA-Interim. Changes in the future have been assessed based on a miniensemble comprising seven different RCM runs. The ensemble comprises different versions of the regional model COSMO-CLM, initial conditions of the driving GCM (ECHAM5/MPI-OM runs 1–3), and two emission scenarios (A1B and B1). Since hail in Germany mainly occurs during the hot months in the late afternoon, we have restricted our investigations to data at 12 UTC (around 12:40 LT in the center of Germany) during the three summer months.

The following major points and conclusions can be inferred from the results obtained:

1. The logistic model approach based on logistic regression essentially improves the diagnostic of hail events through suitable combinations of different hail-related parameters. The model estimates the number of days with an enhanced potential for hail to occur, which is referred to as potential hail index (PHI).

Considering a vast number of meteorological parameters, the following variables are best suited for the logistic hail model: (a) surface-based lifted index at 12 UTC (SLI), (b) minimum near-surface temperature (T_{min}), (c) near-surface temperature (T_{2m}) at 12 UTC, and (d) hail-related and hail-unrelated objective weather types (OWTs) according to the classification of DWD. These four parameters reflect static stability, advection of air masses with specific characteristics such as temperature and moisture, and near-surface properties in the morning and early afternoon. All these conditions are relevant for the development of organized convection in terms of multicells, supercells, or mesoscale convective systems that may produce hail.

2. The PHI obtained by our logistic hail model is in good agreement with insured hail losses and hail signals derived from radar data. The analyses demonstrate that the logistic hail model, calibrated for the federal state of Baden-Württemberg, can be transferred and applied to the whole area of Germany. Only over the northern parts and near the coastline, the results exhibit relatively large uncertainties which limit the validity of the results.
3. Over past decades, the PHI derived from reanalysis shows a markedly north-to-south gradient with the highest hail potential occurring in southern Germany.
4. For the future (2021–2050), six of the seven RCM projections reveal on average an increase in PHI between 10 and 41%. The increase in PHI is statistically significant on the 95% level only in the northwest of Germany and in the very south. The increase in PHI can be ascribed above all to a projected increase in the moisture at low levels caused by the temperature increase, which both result in higher convective energy, and an increase in probability for hail-related weather patterns.
5. In agreement with other studies [e.g., *Hawkins and Sutton*, 2009, 2011], the impact of natural climate variability, which is revealed by the different realizations of the GCM, is the main source of variability in the results of PHI, whereas scenario uncertainty is almost negligible.

A potential weakness of our approach is the neglect of local-scale forced ascent in the LHM. Several studies have shown that convergence zones evolving over topographically structured terrain due to direct thermal circulation, flows around the mountains, or gravity wave formations are decisive for convective initiation [e.g., *van Zomeren and van Delden*, 2007; *Kottmeier et al.*, 2008; *Barthlott et al.*, 2011]. Since orographically induced convergence zones are not well represented by the RCM runs, this effect cannot be considered. Thus, the model results in terms of PHI must be considered as potential for hail formation related to atmospheric characteristics—in accordance to the interpretation of CAPE or SLI. Furthermore, it must be taken into account that the model had been calibrated for the prevailing atmospheric conditions in the federal state of Baden-Württemberg, where hail occurred most frequently compared to other regions in Germany. The results found for that area and the time period considered, however, are in good agreement with those found in other studies on the assessment of hail hazard [*Puskeiler*, 2013], overshooting tops [*Punge et al.*, 2014], or thunderstorm activity in Germany.

Another potential source of uncertainty of our approach may result from the fact that it is based on model data at 12 UTC solely. When air masses with different properties are advected, for example, in conjunction with a frontal passage, atmospheric properties may substantially change during the day. However, hailstorms in Germany have their peak occurrence in the afternoon. *Kunz and Puskeiler* [2010], for example, found that more than 90% of all hailstorms identified by radar analyses within a 12 year period occurred between 13 and 16 UTC. Furthermore, severe hail events typically occur prior to frontal passages. Thus, for the majority of hail events the preconvective environment is well represented by the conditions prevailing at 12 UTC.

The reliability of the LHM approach is, in addition, confirmed by the fact that other studies also have found the applied independent variables to be linked to thunderstorm and hail events [*Willemse*, 1995; *Manzato*, 2003; *Mohr and Kunz*, 2013]. Furthermore, our model did not support the hypothesis that CAPE $\times$ shear is an appropriate predictor for deep moist convection in Germany as stressed by several studies, particularly in the U.S. [e.g., *Brooks et al.*, 2003; *Trapp et al.*, 2007; *Pistotnik et al.*, 2012; *Brooks*, 2013]. This finding is in agreement with other studies on the statistical evaluation of convection in Europe, who found, for instance, that SLI has a higher prediction skill compared to CAPE $\times$ shear [e.g., *Manzato*, 2003; *Kaltenböck et al.*, 2009; *Mohr*, 2013].

For the nest step, we intend to increase the size of our ensemble by integrating the currently performed RCM runs, where meteorological parameters are available on different levels, for example, the new climate simulations of EURO-CORDEX [*Jacob et al.*, 2014]. Most important is to consider model runs performed by different RCMs and GCMs for better assessment of the uncertainties and scope of changes through natural climate variability.

Appendix A: List of Parameter Used

During the development of the logistic hail model different parameters were tested as potential variable/input for the model. A summary of all meteorological parameters which describe the convective, kinematic, or synoptic conditions in the troposphere or the moisture conditions in the lower layer is listed in Table A1.

Table A1. Convective Parameters and Meteorological Parameters Whose Qualities Are Analyzed in the Logistic Hail Model (Equation (4))

Variable x		Meaning	Hail Relevance According to Other Studies	Regions
		Convective Parameters and Indices		
1	CAPE	Convective available potential energy	*Groenemeijer and van Delden* [2007], *Sánchez et al.* [2008], *Xie et al.* [2008], *Hand and Cappelluti* [2011], and *Mohr and Kunz* [2013]	Netherlands, Argentina, China, England, Baden-Württemberg
2	SLI	Lifted index	*Manzato* [2003, 2012], *Kunz* [2007], and *Mohr and Kunz* [2013]	Italy, Baden-Württemberg
3	CIN	Convective inhibition		
4	DCI_S	Deep convective index	*Kunz* [2007] and *Mohr and Kunz* [2013]	Baden-Württemberg
5	$\Delta\theta_E$	Delta θ_e	*Kunz* [2007] and *Mohr and Kunz* [2013]	Baden-Württemberg
6	K	K index	*Sánchez et al.* [2008]	Argentina
7	KO	KO index	*Sánchez et al.* [2009]	France
8	PII	Potential instability index	*Kunz* [2007] and *Mohr and Kunz* [2013]	Baden-Württemberg
9	TT	Total totals	*López et al.* [2007]	Spain
10	VT	Vertical totals	*Piani et al.* [2005]	Turkey
		Moisture Conditions in the Lower Layers		
11	TQV	Precipitable water content	*Billet et al.* [1997], *Piani et al.* [2005], and *Cao* [2008]	USA, Turkey, Canada
12	T_{min}	Minimum temperature in the morning	*Willemse* [1995], *Dessens* [1995], *Sánchez et al.* [1998, 2008], and *Berthet et al.* [2011]	France, Spain, Argentina
13	T_{wet}	Wet-bulb temperature		
14	r_{2m}	Mixing ratio at 2 m		
15	$T_{d,2m}$	Dew point at 2 m		
16	$T_{d,750}$	Dew point at 750 hPa		
17	$T_{d,850}$	Dew point at 850 hPa	*López et al.* [2007] and *Sánchez et al.* [2009]	Spain, France
18	θ_{e850}	Equivalent potential temperature at 850 hPa		
19	MFC	Surface moisture flux convergence	*Banacos and Schultz* [2005] and *van Zomeren and van Delden* [2007]	USA, Western Europe
		Kinematic Conditions		
20	WSh_{0-6}	Magnitude of vector difference between the winds at the surface and 500 hPa	*Brooks et al.* [2003] and *Groenemeijer and van Delden* [2007]	USA, Netherlands
21	WSh_{9-5}	Wind shear like (20) only between 950 and 500 hPa		
22	WSh_{8-5}	Wind shear like (20) only between 850 and 500 hPa		
23		$\sqrt{CAPE} \times WSh_{0-6}$	*Brooks* [2013] and *Pistotnik et al.* [2012]	USA, Europe
24	w_{max}	Maximal vertical wind speed		
25	w_{500}	Vertical wind speed at 500 hPa		
26	w_{700}	Vertical wind speed at 700 hPa	*Kagermazov* [2012]	Caucasus
27	$\mathbf{v}_{H850}$	Horizontal wind speed at 850 hPa	*López et al.* [2007]	Spain
28	$\mathbf{v}_{H500}$	Horizontal wind speed at 500 hPa	*López et al.* [2007]	Spain
		Synoptic Conditions		
29	OWT	Weather types	*Aran et al.* [2010], *García-Ortega et al.* [2011], and *Kapsch et al.* [2012]	Spain, Baden-Württemberg
30	ζ_{500}	Relative vorticity at 500 hPa		
31	NGH	Freezing level height	*Billet et al.* [1997], *Xie et al.* [2008], and *Sánchez et al.* [2009]	USA, China, France
32	PS	Surface pressure	*Sánchez et al.* [2008]	Argentina

Table A1. (continued)

	Variable x	Meaning	Hail Relevance According to Other Studies	Regions
		Other Parameters		
33	T_{con}	Convective temperature		
34	T_{2m}	Surface temperature		
35	$RAIN_{CON}$	Convective precipitation		
36	$RAIN_{GSP}$	Total between ipitation		
37	FI_{10-5}	Thickness between 1000 and 500 hPa		

Acknowledgments

This work was funded by the "Stiftung Umwelt und Schadenvorsorge" of the SV SparkassenVersicherung, which we want to thank. The CCLM-IMK simulations have been performed by the Institute for Meteorology and Climate Research (IMK-TRO), Karlsruhe Institute of Technology (KIT), Germany (http://www.imk-tro.kit.edu). The CCLM-Consortium Runs has been obtained from the Climate and Environmental Retrieval and Archive (CERA) of the Deutsche Klimarechenzentrum (DKRZ) Hamburg, Germany (http://cera-www.dkrz.de), and the BTUInt from one of the coauthors (Keuler; http://www.euro-cordex.net/EURO-CORDEX-Data.2613.0.html). The lightning data were provided by the lightning information service BLitz InformationDienst Siemens (BLIDS), Karlsruhe, Germany (http://blids.de). The insurance data to support this article are from the building insurance company SV SparkassenVersicherung and from the agricultural insurance company Vereinigte Hagel, which we want to thank. Only these two data sets are confidential and cannot be provided to others. The hail signals are based on the radar data from the German Weather Service (DWD; http://www.dwd.de/radar). Special thanks go to Marc Puskeiler for the processing and provision of the hail information and to Marie Kapsch for the processing and provision of the objective weather types from the CCLM-IMK and CCLM-Consortium Runs simulations. We thank the IMK-TRO working group "Water cycle and Climate Modeling," namely, Peter Berg, Hendrik Feldmann, Hans-Jürgen Panitz, and Gerd Schädler, for various support. Helpful comments and constructive suggestions from four anonymous reviewers substantially improved the quality of this paper.

References

Applequist, S., G. Gahrs, R. L. Pfeffer, and X. F. Niu (2002), Comparison of methodologies for probabilistic quantitative precipitation forecasting, *Weather Forecasting*, *17*, 783–799.

Aran, M., J. C. Pena, and M. Torá (2010), Atmospheric circulation patterns associated with hail events in Lleida (Catalonia), *Atmos. Res.*, *100*, 428–438.

Backhaus, K., B. Erichson, W. Plinke, and R. Weiber (2011), *Multivariate Analysemethoden: Eine Anwendungsorientierte Einführung*, 583 pp., Springer, Heidelberg, Germany.

Banacos, P. C., and D. M. Schultz (2005), The use of moisture flux convergence in forecasting convective initiation: Historical and operational perspectives, *Weather Forecasting*, *20*, 351–366.

Barthlott, C., et al. (2011), Initiation of deep convection at marginal instability in an ensemble of mesoscale models: A case-study from COPS, *Q. J. R. Meteorol. Soc.*, *137*, 118–136.

Berg, P., S. Wagner, H. Kunstmann, and G. Schädler (2013), High resolution RCM simulations for Germany: Part I—Validation, *Clim. Dyn.*, *1–2*, 1–14.

Berthet, C., J. Dessens, and J. L. Sanchez (2011), Regional and yearly variations of hail frequency and intensity in France, *Atmos. Res.*, *100*, 391–400.

Billet, J., M. DeLisi, B. G. Smith, and C. Gates (1997), Use of regression techniques to predict hail size and the probability of large hail, *Weather Forecasting*, *12*, 154–164.

Bissolli, P., and E. Dittmann (2001), The objective weather type classification of the German Weather Service and its possibilities of application to environmental and meteorological investigations, *Meteorol. Z.*, *10*, 253–260.

Bissolli, P., J. Grieser, N. Dotzek, and M. Welsch (2007), Tornadoes in Germany 1950–2003 and their relation to particular weather conditions, *Global Planet. Change*, *57*, 124–138.

Brooks, H. E. (2013), Severe thunderstorms and climate change, *Atmos. Res.*, *123*, 129–138.

Brooks, H. E., J. W. Lee, and J. P. Craven (2003), The spatial distribution of severe thunderstorm and tornado environments from global reanalysis data, *Atmos. Res.*, *67*, 73–94.

Cao, Z. (2008), Severe hail frequency over Ontario, Canada: Recent trend and variability, *Geophys. Res. Lett.*, *35*, L14803, doi:10.1029/2008GL034888.

Changnon, S. A. (1970), Hailstreaks, *J. Atmos. Sci.*, *27*, 109–125.

Dee, D. P., et al. (2011), The ERA-Interim reanalysis: Configuration and performance of the data assimilation system, *Q. J. R. Meteorol. Soc.*, *137*(656), 553–597.

Dessens, J. (1995), Severe convective weather in the context of a nighttime global warming, *Geophys. Res. Lett.*, *22*, 1241–1244.

Dittmann, E. (1995), *Berichte des Deutschen Wetterdienstes. Bd. 197: Objektive Wetterlagenklassifikation*, 41 pp., Deutscher Wetterdienst (DWD), Offenbach, Germany.

Dotzek, N., P. Groenemeijer, B. Feuerstein, and A. M. Holzer (2009), Overview of ESSL's severe convective storms research using the European Severe Weather Database ESWD, *Atmos. Res.*, *93*, 575–586.

Eccel, E., P. Cau, K. Riemann-Campe, and F. Biasioli (2012), Quantitative hail monitoring in an alpine area: 35-year climatology and links with atmospheric variables, *Int. J. Climatol.*, *32*, 503–517.

Galway, J. G. (1956), The lifted index as a predictor of latent instability, *Bull. Am. Meteorol. Soc.*, *37*, 528–529.

García-Ortega, E., L. López, and J. L. Sánchez (2011), Atmospheric patterns associated with hailstorm days in the Ebro Valley, Spain, *Atmos. Res.*, *100*, 401–427.

Gessler, S. E., and S. E. Patty (2013), *Forensic Engineering: Damage Assessments for Residential and Commercial Structures*, pp. 23–67 Petty, S. E. (ed), Hail Fundamentals and General Hail-strike Damage Assessment Methodology, CRC Press, Boca Raton, Fla.

Giaiotti, D., S. Nordio, and F. Stel (2003), The climatology of hail in the plain of Friuli Venezia Giulia, *Atmos. Res.*, *67*, 247–259.

Götze, W., C. Deutschmann, and H. Link (2002), *Statistik. Managementwissen für Studium und Praxis*, 475 pp., Oldenbourg Wissenschaftsverlag, Munic, Germany.

Groenemeijer, P. H., and A. van Delden (2007), Sounding-derived parameters associated with large hail and tornadoes in the Netherlands, *Atmos. Res.*, *83*, 473–487.

Haklander, A. J., and A. van Delden (2003), Thunderstorm predictors and their forecast skill for the Netherlands, *Atmos. Res.*, *67–68*, 273–299.

Hamill, T. M., and J. Juras (2006), Measuring forecast skill: Is it real skill or is it the varying climatology?, *Q. J. R. Meteorol. Soc.*, *132*, 2905–2923.

Hand, W. H., and G. Cappelluti (2011), A global hail climatology using the UK Met Office convection diagnosis procedure (CDP) and model analyses, *Meteorol. Appl.*, *18*, 446–458.

Hawkins, E., and R. Sutton (2009), The potential to narrow uncertainty in regional climate predictions, *Bull. Am. Meteorol. Soc.*, *90*, 1095–1107.

Hawkins, E., and R. Sutton (2011), The potential to narrow uncertainty in projections of regional precipitation change, *Clim. Dyn.*, *37*, 407–418.

Hollweg, H. D., et al. (2008), Ensemble simulations over Europe with the regional climate model CLM forced with IPCC AR4 global scenarios, *Tech. Rep., 3*, Modelle & Daten (M & D), Hamburg, Germany. p. 152.

Hosmer, D. W., and S. Lemeshow (2000), *Applied Logistic Regression*, 392 pp., vol. 354, Wiley–Interscience, New York.

Huntrieser, H., H. H. Schiesser, W. Schmid, and A. Waldvogl (1997), Comparison of traditional and newly developed thunderstorm indices for Switzerland, *Weather Forecasting*, *12*, 108–125.

Jacob, D., et al. (2014), EURO-CORDEX: New high-resolution climate change projections for European impact research, *Reg. Environ. Change*, *14*, 563–578.

Jolliffe, I. T., and D. B. Stephenson (2012), *Forecast Verification: A Practitioner's Guide in Atmospheric Science*, 240 pp., John Wiley, Chichester, England.

Kagermazov, A. K. (2012), The forecast of hail based on the atmospheric global model (T254 NCEP) output data, *Russ. Meteorol. Hydrol.*, *37*, 165–169.
Kaltenböck, R., G. Diendorfer, and N. Dotzek (2009), Evaluation of thunderstorm indices from ECMWF analyses, lightning data and severe storm reports, *Atmos. Res.*, *93*, 381–396.
Kapsch, M. L., M. Kunz, R. Vitolo, and T. Economou (2012), Long-term trends of hail-related weather types in an ensemble of regional climate models using a Bayesian approach, *J. Geophys. Res.*, *117*, D15107, doi:10.1029/2011JD017185.
Knight, D., and N. Knight (2003), *Encyclopedia of Atmospheric Sciences*, pp. 924–929, Hail and Hailstorms, Academic Press Inc., USA.
Kotlarski, S., et al. (2014), Regional climate modeling on European scales: A joint standard evaluation of the EURO-CORDEX RCM ensemble, *Geosci. Model Dev. Discuss.*, *7*, 217–293.
Kottmeier, C., et al. (2008), Mechanisms initiating deep convection over complex terrain during COPS, *Meteorol. Z.*, *17*, 931–948.
Kunz, M. (2007), The skill of convective parameters and indices to predict isolated and severe thunderstorms, *Nat. Hazards Earth Syst. Sci.*, *7*, 327–342.
Kunz, M., and M. Puskeiler (2010), High–resolution assessment of the hail hazard over complex terrain from radar and insurance data, *Meteorol. Z.*, *19*, 427–439.
Kunz, M., J. Sander, and C. Kottmeier (2009), Recent trends of thunderstorm and hailstorm frequency and their relation to atmospheric characteristics in southwest Germany, *Int. J. Climatol.*, *29*, 2283–2297.
Lee, J. W. (2002), Tornado proximity soundings from the NCEP/NCAR reanalysis data, PhD thesis, Univ. of Okla., Norman. p. 61.
López, L., E. García-Ortega, and J. L. Sánchez (2007), A short-term forecast model for hail, *Atmos. Res.*, *83*, 176–184.
Manzato, A. (2003), A climatology of instability indices derived from Friuli Venezia Giulia soundings, using three different methods, *Atmos. Res.*, *67*, 417–454.
Manzato, A. (2007), A note on the maximum Peirce Skill Score, *Weather Forecasting*, *22*, 1148–1154.
Manzato, A. (2012), Hail in Northeast Italy: Climatology and bivariate analysis with the sounding-derived indices, *J. Appl. Meteorol. Climatol.*, *51*, 449–467.
McKelvey, R. D., and W. Zavoina (1975), A statistical model for the analysis of ordinal level dependent variables, *J. Math. Socio.*, *4*, 103–120.
Mironov, D., E. Heise, E. Kourzeneva, B. Ritter, N. Schneider, and A. Terzhevik (2010), Implementation of the lake parameterisation saheme FLake into the numerical weather prediction model COSMO, *Boreal Environ. Res.*, *15*, 218–230.
Mohr, S. (2013), Änderung des Gewitter- und Hagelpotentials im Klimawandel, Wiss. Berichte d. Instituts für Meteorologie und Klimaforschung des Karlsruher Instituts für Technologie Band 58, Karlsruhe, Germany, 243 pp.
Mohr, S., and M. Kunz (2013), Recent trends and variabilities of convective parameters relevant for hail events in Germany and Europe, *Atmos. Res.*, *123*, 211–228.
Munich Re (2014), *TOPICS GEO: Natural catastrophes 2013 Analyses, assessments, positions*, Munchener Ruckversicherungs-Gesellschaft, Munich, Germany. [Available at http://www.munichre.com/site/corporate/get/documents_E1043212252/mr/assetpool.shared/Documents/5_Touch/_Publications/302-08121_en.pdf.]
Nakićenović, N., et al. (2000), *IPCC Special Report on Emissions Scenarios*, pp. 1–27, Cambridge Univ. Press, Cambridge, U. K., and New York.
O'Brien, R. M. (2007), A caution regarding rules of thumb for variance inflation factors, *Qual. Quant.*, *41*, 673–690.
Piani, F., A. Crisci, G. de Chiara, G. Maracchi, and F. Meneguzzo (2005), Recent trends and climatic perspectives of hailstorms frequency and intensity in Tuscany and Central Italy, *Nat. Hazards Earth Syst. Sci.*, *5*, 217–224.
Pistotnik, G., P. Groenemeijer, K. Riemann-Campe, and T. Kühne (2012), STEPCLIM: Severe Thunderstorm Evaluation and Predictability in Climate Models, *26th Conference on Severe Local Storms, 5–8 November 2012, Nashville, USA*.
Pruppacher, H. R., and J. D. Klett (1997), *Microphysics of Clouds and Precipitation*, 954 pp., vol. 18, Kluwer Acad., Dordrecht, Netherlands.
Punge, H. J., K. M. Bedka, M. Kunz, and A. Werner (2014), A new physically based stochastic event catalog for hail in Europe, *Nat. Hazards*, *73*, 1625–1645.
Puskeiler, M. (2013), Radarbasierte Analyse der Hagelgefährdung in Deutschland, Wiss. Berichte d. Instituts für Meteorologie und Klimaforschung des Karlsruher Instituts für Technologie Band 59, Karlsruhe, Germany, 202 pp.
Rockel, B., A. Will, and A. Hense (2008), The regional climate model COSMO-CLM (CCLM), *Meteorol. Z.*, *17*, 347–348.
Roeckner, E., et al. (2003), The atmospheric general circulation model ECHAM 5. Part I: Model description. *MPI-Report, Hamburg, Germany*, *249*, 127.
Sánchez, J. L., R. Fraile, M. T. De la Fuente, and J. L. Marcos (1998), Discriminant analysis applied to the forecasting of thunderstorms, *Meteorol. Atmos. Phys.*, *68*, 187–195.
Sánchez, J. L., L. López, C. Bustos, J. L. Marcos, and E. García-Ortega (2008), Short-term forecast of thunderstorms in Argentina, *Atmos. Res.*, *88*, 36–45.
Sánchez, J. L., J. L. Marcos, J. Dessens, L. López, C. Bustos, and E. García-Ortega (2009), Assessing sounding-derived parameters as storm predictors in different latitudes, *Atmos. Res.*, *93*, 446–456.
Schädler, G., P. Berg, D. Düthmann, H. Feldmann, J. Ihringer, H. Kunstmann, J. Liebert, B. Merz, I. Ott, and S. Wagner (2012), *Flood Hazards in a Changing Climate—Project Report*, 83 pp., Center for Disaster Management and Risk Reduction Technology (CEDIM), Karlsruhe, Germany.
Schiesser, H. H. (2003), Hagel, in *Extremereignisse und Klimaänderung*, pp. 65–68, Organe consultatif sur les changements climatiques (OcCC), Bern, Swiss.
Schmeits, M. J., K. J. Kok, and D. H. P. Vogelezang (2005), Probabilistic forecasting of (severe) thunderstorms in the Netherlands using model output statistics, *Weather Forecasting*, *20*, 134–148.
Trapp, R. J., N. S. Diffenbaugh, H. E. Brooks, M. E. Baldwin, E. D. Robinson, and J. S. Pal (2007), Changes in severe thunderstorm environment frequency during the 21st century caused by anthropogenically enhanced global radiative forcing, *Proc. Natl. Acad. Sci.*, *104*, 19,719–19,723.
Uppala, S. M., et al. (2005), The ERA-40 re-analysis, *Q. J. R. Meteorol. Soc.*, *131*, 2961–3012.
van Zomeren, J., and A. van Delden (2007), Vertically integrated moisture flux convergence as a predictor of thunderstorms, *Atmos. Res.*, *83*, 435–445.
Vautard, R., et al. (2013), The simulation of European heat waves from an ensemble of regional climate models within the EURO-CORDEX project, *Clim. Dyn.*, *41*(9-10), 2555–2575.
Wagner, S., P. Berg, G. Schädler, and H. Kunstmann (2013), High resolution RCM simulations for Germany: Part II—Projected climate changes, *Clim. Dyn.*, *40*, 415–427.
Waldvogel, A., B. Federer, and P. Grimm (1979), Criteria for the detection of hail cells, *J. Appl. Meteorol.*, *18*, 1521–1525.
Wilks, D. S. (2006), *Statistical Methods in the Atmospheric Sciences*, 627 pp. 2nd ed., Academie Press, Elsevier, Burlington, USA.
Willemse, S. (1995), A statistical analysis and climatological interpretation of hailstorms in Switzerland, Doctor of Natural Science thesis dissertation No. 11137, Swiss Federal Institute of Technology, Zurich, Swiss. 189 pp.
Xie, B., Q. Zhang, and Y. Wang (2008), Trends in hail in China during 1960–2005, *Geophys. Res. Lett.*, *35*, L13801, doi:10.1029/2008GL034067.